

Systematic study of precompound neutron emission in α -particle-induced reactions

Manoj Kumar Sharma,^{1,*} Mahesh Kumar,¹ Mohd. Shuaib,² Vijay Raj Sharma,³ Abhishek Yadav,⁴
Pushpendra P. Singh,⁵ B. P. Singh,^{2,†} and R. Prasad²

¹*Department of Physics, Shri Varsheny College, Aligarh (UP)-202 001, India*

²*Department of Physics, Aligarh Muslim University, Aligarh-202002, India*

³*Departamento de Aceleradores, Instituto Nacional de Investigaciones Nucleares, Apartado Postal 18-1027,
C.P. 11801 Ciudad de Mexico, Mexico*

⁴*Inter University Accelerator Centre, New Delhi, India*

⁵*Department of Physics, Indian Institute of Technology, Ropar Rupnagar 140001, Punjab, India*



(Received 26 July 2018; revised manuscript received 18 September 2018; published 9 November 2018)

Background: The precompound emission process in light-ion fusion interactions has been a topic of considerable interest to nuclear physicists for many years. Although widespread theoretical and experimental efforts have been devoted to understand the reaction dynamics of precompound emission, no systematic study has been carried out to determine the driving input parameters in such reactions.

Purpose: The importance of this study has large impact on reaction dynamics. In order to get parameters describing the precompound emission, excitation functions have been measured by using an α -particle beam on ^{141}Pr target nuclei. Further, a sensitive analysis of excitation functions has been performed to investigate the systematics of the precompound process with mass number of target nuclei.

Method: The off-line γ -ray-spectrometry-based activation technique has been used for the measurement of the excitation functions. The presently measured excitation functions on the system $\alpha + ^{141}\text{Pr}$ (and those experimental values taken from literature on the $\alpha + ^{51}\text{V}$, $\alpha + ^{55}\text{Mn}$, $\alpha + ^{93}\text{Nb}$, $\alpha + ^{121}\text{Sb}$, and $\alpha + ^{123}\text{Sb}$ systems) have been analyzed within the framework of compound and precompound emissions by using model code ALICE.

Results: The analysis performed by using code ALICE with the same set of precompound parameters indicates that the experimentally measured excitation functions could be reproduced only when the precompound emission, simulated theoretically, has been taken into account. The influence of various important precompound parameters of the code ALICE with their physically accepted values for these systems has been judged and a systematics on precompound emission process is achieved with mass number of the target nuclei.

Conclusions: The developed systematics for α -induced reactions on target nuclei: ^{51}V , ^{55}Mn , ^{93}Nb , ^{121}Sb , ^{123}Sb , and ^{141}Pr indicates that the precompound process is governed by the excitation energy available to the nucleons at the surface the composite systems. Furthermore, mass number of the target nuclei may also play an important role in precompound process at low projectile energies.

DOI: [10.1103/PhysRevC.98.054607](https://doi.org/10.1103/PhysRevC.98.054607)

I. INTRODUCTION

The presence of precompound nucleus (PCN) along with compound-nucleus (CN) emission mechanism has been established within both the theoretical and experimental aspects in light-ion-induced reactions [1–9]. It has been well established that with increase in excitation energy, the PCN mechanism may even become the dominant process in which emission of primary particles [neutrons (n), protons (p), and alpha particles (α)] takes place during the process of energy sharing inside the composite nucleus, just after the first projectile-target interaction and well before the establishment of thermodynamical equilibrium. These emitted particles are called precompound particles and the phenomenon is known

as precompound emission [10–17]. The key role of precompound emission in reaction dynamics is that it reflects the dynamics of formation of an excited composite system and its evolution to the equilibrium states leading to the formation of a compound-nucleus [18,19].

Some of the important experimental characteristics of the precompound process over compound nucleus process are (i) the presence of a larger number of high-energy particles as compared to the spectrum predicted by the statistical (i.e., CN) model [20], (ii) forward-peaked angular distribution of the emitted particles through PCN process [21], (iii) observation of smaller recoil range/linear momentum of the reaction residues left after emission of precompound particles as compared to CN particles [22], (iv) observation of lower value of the spin with precompound process as compared to compound nucleus process [22], (v) slowly decreasing tails

*Corresponding author: manojamu76@gmail.com

†bpsinghamu@gmail.com

of the excitation functions (EFs) [1,12,23], and (vi) stretched particle distribution in angular momentum space [24–26].

There are many experimental methods used to distinguish the precompound emission process from compound nucleus process. It may be studied by measuring particle (n , p , and α) spectra in the time-of-flight experiments in coincidence with characteristic γ rays of specific reaction residues [27]. The γ -ray multiplicity experiments may also provide a sensitive method of detecting deviations from compound-nucleus formation and decay in terms of precompound process [28,29]. Furthermore, it may be studied by measuring the difference in the flux of emitted particles in the forward direction over the backward direction. Another method often employed is to analyze the measured excitation functions for deviations from the statistical model predictions. It may be emphasized here that the influence of precompound emission over compound-nucleus mechanism, particularly at the low incident energies is more interesting, since theoretically it is expected to occur at relatively higher projectile energies [1]. Thus, the study of measurement and analysis of excitation functions is one of the best experimental methods to provide a better insight to the energy dependent precompound process over compound-nucleus process. The features of the excitation functions at the low, medium, and high energies may give information about the reaction mechanism involved. The low-energy portion of the excitation functions is dominated by the compound-nucleus mechanism, however, with the increase in projectile energy, the strength of the precompound processes becomes relatively more [1,7,8,15,30–33]. As such, the study of EFs may give information of considerable value about the precompound emission process. Though, a large amount of data on the PCN emission is available in literature, but there is no systematic study on how the competition between the precompound and the compound nucleus emission processes depends on the change in the target mass and the variation of the excitation energy.

With a view to study the precompound and compound-nucleus processes, several authors [1,7,8,12,15,30,34] measured the EFs for the reaction residues produced in the interaction of proton and α -particle beams with the target nuclei covering a wide mass region. The analysis of these excitation functions have been performed only with the aim to study the reaction dynamics other than the compound-nucleus process. A large amount of experimental data on measurements of the excitation functions for α -induced reaction on several target nuclei exists in literature. Although the data of charged-particle-induced reactions on excitation functions measurements had been used either for the production of specific radionuclide for medical purposes or in accelerator-driven subcritical (ADS) reactors [35]. The work reported in this paper has been performed as a part of our ongoing program of the measurement and analysis of cross-section data in light- and heavy-ion-induced reactions [1,7,8,12,17,22,23,36–39]. The present work is an attempt to investigate a systematics of precompound emission at low projectile energies in α -induced reactions, where the probability of emission of a single neutron through PCN process is higher as compared to the reactions leading to the emission of more than one particle through pn , $p2n$, and $2pn$ reaction channels.

With this motivation, to study the precompound process in a unified, consistent, and systematic way, the excitation function for reaction $^{141}\text{Pr}(\alpha, n)^{144}\text{Pm}$ has been measured by using the stacked foil activation technique in the energy range $\approx 14\text{--}40$ MeV. Further, the experimental data on EFs for reactions $^{51}\text{V}(\alpha, n)^{54}\text{Mn}$ [34,40,41], $^{55}\text{Mn}(\alpha, n)^{58m+g}\text{Co}$ [42], $^{93}\text{Nb}(\alpha, n)^{96}\text{Tc}$ [12], $^{121}\text{Sb}(\alpha, n)^{124}\text{I}$ [1,43,44], and $^{123}\text{Sb}(\alpha, n)^{126}\text{I}$ [1,43,44] measured earlier by our group or others have been taken and analyzed with code ALICE [45]. The code ALICE includes both the compound-nucleus and the precompound emission processes. The compound-nucleus calculations in this code are performed using the Weisskopf-Ewing model [46] while the precompound component is simulated using the geometry dependent hybrid model [47]. It may be pointed out that the targets chosen for the present study are odd- Z and odd- A nuclei in order to minimize the ambiguity, if any, arising due to odd even effect of the targets.

This paper is organized as follows. The experimental details of the measurement of EFs for system $\alpha + ^{141}\text{Pr}$ are given in the Sec. II, while, Sec. III deals with the analysis of the measured excitation functions with code ALICE [45]. A brief discussion on the measurement and analysis of the earlier data within the framework of precompound emission theory is given in Sec. IV. Section V of this paper deals with the driving precompound parameters and investigation of a systematics with mass number of target nuclei. The results of the present analysis are summarized in the conclusion, Sec. VI of this paper.

II. EXPERIMENTAL

The experiments have been carried out at the Variable Energy Cyclotron Centre (VECC), Kolkata, India, using a collimated α -particle beam of ≈ 40 MeV. The samples of natural praseodymium ^{141}Pr (of purity 99.9%) having thickness ≈ 3.32 mg/cm² were used as the targets. The targets were prepared employing vacuum evaporation technique by depositing ^{141}Pr on Al foils of thickness ≈ 6.75 mg/cm². The Al foils serve as energy degrader as well as catcher/backing foils, where the recoiling residues from the composite system may be trapped. The thickness of each target sample/Al catcher was determined precisely prior to its use in the stack by α -transmission method, which is based on the measurement of the energy lost by 5.487 MeV α particles, obtained from standard ^{241}Am source, while passing through the target material. In the stacked foil activation technique, the energetic beam traverses through the samples with degrading beam energies. Thus, it is possible to bombard several samples of the stack at different energies in a single irradiation.

In the present experiments, a stack consisting of eight ^{141}Pr target samples followed by Al degraders/catchers was irradiated for ≈ 12 h. The beam current ≈ 100 nA was monitored from the current integrator count rate. The calculations for average beam energy on a given target of the stack have been performed using the stopping power program SRIM [48]. After irradiation, the stack consisting of eight samples was dismantled and activities induced in each sample were measured separately and followed for several weeks by using a high-resolution large volume (100 c.c.) high-purity germanium

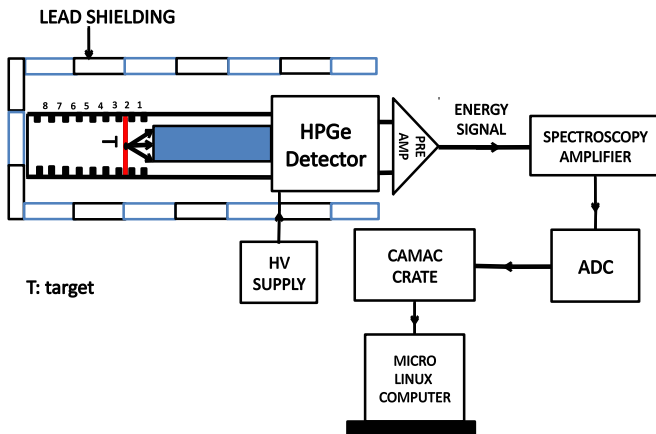


FIG. 1. A typical block diagram of γ -ray spectrometer setup along with source-detector arrangements.

(HPGe) detector coupled to an ORTEC's PC-based multi-channel analyzer. An illustration of how the irradiated target is mounted with respect to the detector is shown in Fig. 1. In the present work, a ^{152}Eu point γ source is used to determine the efficiency of HPGe detector. The geometry-dependent efficiency (G_ε) of HPGe detector for different source-detector separations was estimated using the following relation;

$$G_\varepsilon = \frac{N_0}{N_{a0}\theta e^{-\lambda t}}, \quad (1)$$

where N_0 , is the observed disintegration rate of the standard source at the time of measurement, N_{a0} is the disintegration rate at the time of manufacture, λ is the decay constant, t is the lapse time between the manufacture of the source and the start of counting, θ is the branching ratio of the characteristic γ rays. As a representative case, the measured geometry-dependent efficiency obtained by using Eq. (1) as a function of γ -ray energies is shown in Fig. 2. The resolution of HPGe detector was ≈ 2 keV for 1332 keV γ line of ^{60}Co . During the counting of the samples, the sample-detector

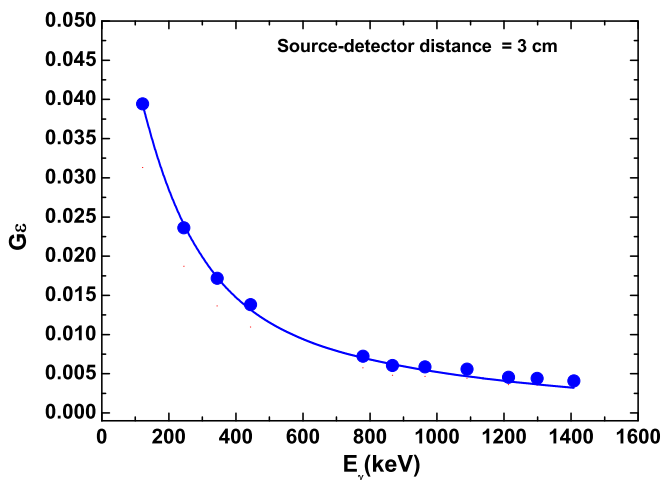


FIG. 2. The measured geometry-dependent efficiency as a function of γ -ray energies.

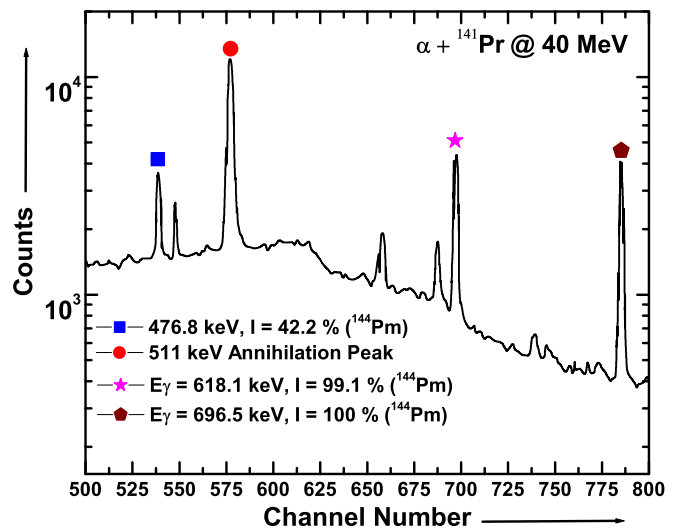


FIG. 3. A typical γ -ray spectrum of the irradiated sample at 40 MeV.

distances are suitably adjusted in order to minimize the dead time to $<10\%$. The residual nuclei produced in the $\alpha + ^{141}\text{Pr}$ system have been identified by their characteristic γ rays and their measured half-lives. A typical γ -ray spectrum of the irradiated sample at 40 MeV is shown in Fig. 3. The pertinent decay data such as half-life, characteristic γ lines and their intensities, used in the present work for the yield calculations have been taken from Refs. [49,50] and are given in Table I. The measured intensities of the characteristic γ lines of the identified reaction residues ^{144}Pm have been used to calculate the cross sections for the corresponding reaction channels employing a FORTRAN program based on standard formulations [17],

$$\sigma_r(E) = \frac{C_a \lambda \exp(\lambda t_i)}{N_o \phi P K(G_\varepsilon) [1 - \exp(-\lambda t_i)] [1 - \exp(-\lambda t_a)]}, \quad (2)$$

where, C_a is the observed counts during the accumulation time t_a of the induced activity of decay constant λ , N_o the number of target nuclei irradiated for time t_i with a particle beam of flux ϕ , t_i the time lapse between the stop of irradiation and the start of counting, P the branching ratio of the characteristic γ ray and G_ε the geometry-dependent efficiency of the detector for the γ ray of a given energy. The value of G_ε depends on the energy of the γ ray and also on the relative separation between the source and detector. In order to determine the

TABLE I. Identified γ -rays, intensity, Q value, and half-life of reaction residues ^{144}Pm .

Reaction channel	Q value (MeV)	Half-life	E_γ (keV)	Intensity (%)
$^{141}\text{Pr}(\alpha, n)$	-10.25	363 d	476.8	42.2
			618.1	99.1
			696.5	100.0

value of G_ϵ for γ rays of different energies, a standard source of ^{152}Eu of known strength was used, as mentioned earlier. As such, proper correction for the geometry-dependent efficiency has been taken into account for each case. The factor $[1 - \exp(-\lambda t_i)]$, known as the saturation correction takes care of the decay of evaporation residues during the irradiation. The corrections for the decay of the induced activity due to the delay between the stop of irradiation and the start of counting and during the data accumulation are taken into account via the factors $\exp(\lambda t_i)$ and $[1 - \exp(-\lambda t_a)]$, respectively. The factor $K\{=[1 - \exp(-\mu x)]/\mu x\}$ is the correction for the self-absorption of the γ radiation in the sample thickness itself, where x is the thickness of the sample and μ is the γ -ray absorption coefficients taken from Ref. [51].

A critical evaluation of uncertainties in the measured cross sections has been considered and is estimated to be $<10\%$. The errors in the measured cross sections may arise due to (i) nonuniform deposition of the target material and inaccurate estimate of the foil thickness which may be $\leq 1\%$, (ii) during the irradiations, fluctuations in the beam current may result in the variation of the incident flux. Many tests were performed to check the time-integrated beam fluctuations and it was estimated that beam fluctuations may introduce errors of not more than 5% in the measured cross sections, (iii) uncertainty in the determination of the geometry-dependent efficiency of the γ -ray spectrometer may give rise to error in the production cross sections. Further, the uncertainty in determining the efficiency of the spectrometer may also appear due to the solid-angle effect, as the irradiated samples were not point sources like the standard source, but had a finite diameter, which may be $\leq 5\%$, (iv) the product nuclei recoiling out of the thin target may introduce large errors in the measured cross sections. This was minimized as the catcher/backing foils used in the stack for irradiation were of sufficient thickness to stop even the most energetic recoiling residues.

III. ANALYSIS OF EXCITATION FUNCTIONS

The code ALICE developed by Blann [45], has been used to calculate the compound nucleus and the precompound emission cross sections. The CN calculation is performed by using the Weisskopf-Ewing model [46], while, the PCN component is simulated by employing the geometry dependent hybrid (GDH) model [47]. The emissions of neutron, proton, deuteron, and/or α particles are considered in this code. The Myers-Swiatecki/Lysekil mass formula [52] is used for calculating the Q values and the binding energies of all the nuclei in the evaporation chain. The calculations for the PCN emission in this code are performed assuming equipartition of energy among initially excited particles and holes. The mean-free path (MFP) for intranuclear transition rates may be calculated either from the optical potential parameters of Becchetti and Greenlees [53] or from Pauli corrected nucleon-nucleon cross sections [54,55]. In the present calculations, the optical potentials of Becchetti and Greenlees [53] have been used.

In this code, the level density parameter a , the initial exciton number n_0 , and the mean-free path multiplier COST are some of the important parameters. The level density parameter

a mainly affects the CN component, while the initial exciton number n_0 and the mean-free path multiplier COST govern the PCN component. The physical description of these parameters and their effects on measured EFs are also important to be discussed. The nuclear level density is defined as the number of nuclear states per excitation energy interval, realized as a specific pattern of single-particle excitations, at a given excitation energy. Level densities of the residue in code ALICE may be calculated either from the Fermi gas model or from the constant temperature form. In the present work, the Fermi gas model is used to calculate the nuclear level density [56] as;

$$\rho(E) = (E - \delta)^{-5/4} \exp[2\sqrt{a(E - \delta)}], \quad (3)$$

where, δ is the pairing term and E is the excitation energy of the nucleus. In the present calculations, the level density parameter a is calculated using the expression $a = A/K$, where A is the mass number and K is a free parameter, which may be varied to fit the experimental data. Calculations were performed for different values of parameter $K = 8, 9$, and 10 for reaction $^{141}\text{Pr}(\alpha, n)^{144}\text{Pm}$ and are shown in Fig. 4(a). As can be seen from this figure, there is a little influence of the parameter K on the measured excitation functions. As such, in the present work, $K = 8$ (default value in code ALICE) has been considered for calculations and found to satisfactorily reproduce the experimental data for the presently studied reactions. This value of $K = 8$ is also in accordance with Dilg *et al.* [57].

Further, in the geometry dependent hybrid model, the intermediate states of a nuclear system are characterized by the excitation energy E^* and the number n_p of excited particles and n_h of excited holes. The particles and holes are defined relative to the ground state of the nucleus and are called excitons. The initial configuration of the compound system defined by the exciton number $n_0 = (n_p + n_h)$ is a crucial parameter of the PCN formalism that determines the shape of EFs in the higher-energy region. In order to get an actual value of the initial exciton number n_0 , the calculations for different values of n_0 ranging from 4–6 with configurations $(2p + 2n + 0h)$ for $n_0 = 4$, $(3p + 2n + 0h)$ for $n_0 = 5$ and $(3p + 2n + 1h)$ for $n_0 = 6$, respectively, have been performed for reaction $^{141}\text{Pr}(\alpha, n)^{144}\text{Pm}$ and is shown in Fig. 4(b). It may be observed from Fig. 4(b), that a value of initial exciton number $n_0 = 4$ fits the experimental data satisfactorily over the entire range of energies. A value of initial exciton number $n_0 = 4$ for α -induced reactions is justified [47]. The lower value of initial exciton number n_0 gives larger PCN contribution. It is because of the fact that the lower value of n_0 means larger number of two-body interactions prior to the establishment of thermodynamic equilibrium, resulting in larger precompound contribution.

The mean-free path multiplier COST is another important parameter in code ALICE for PCN formalism that accounts for difference, if any, between the calculated and actual mean-free paths for two body residual interactions and is used to adjust the nuclear mean-free path in order to reproduce the experimental data. The effect of variation of parameter COST i.e., COST= 0 and COST= 2 on calculated EF for the reaction $^{141}\text{Pr}(\alpha, n)^{144}\text{Pm}$ is shown in Fig. 4(c). As can be seen from

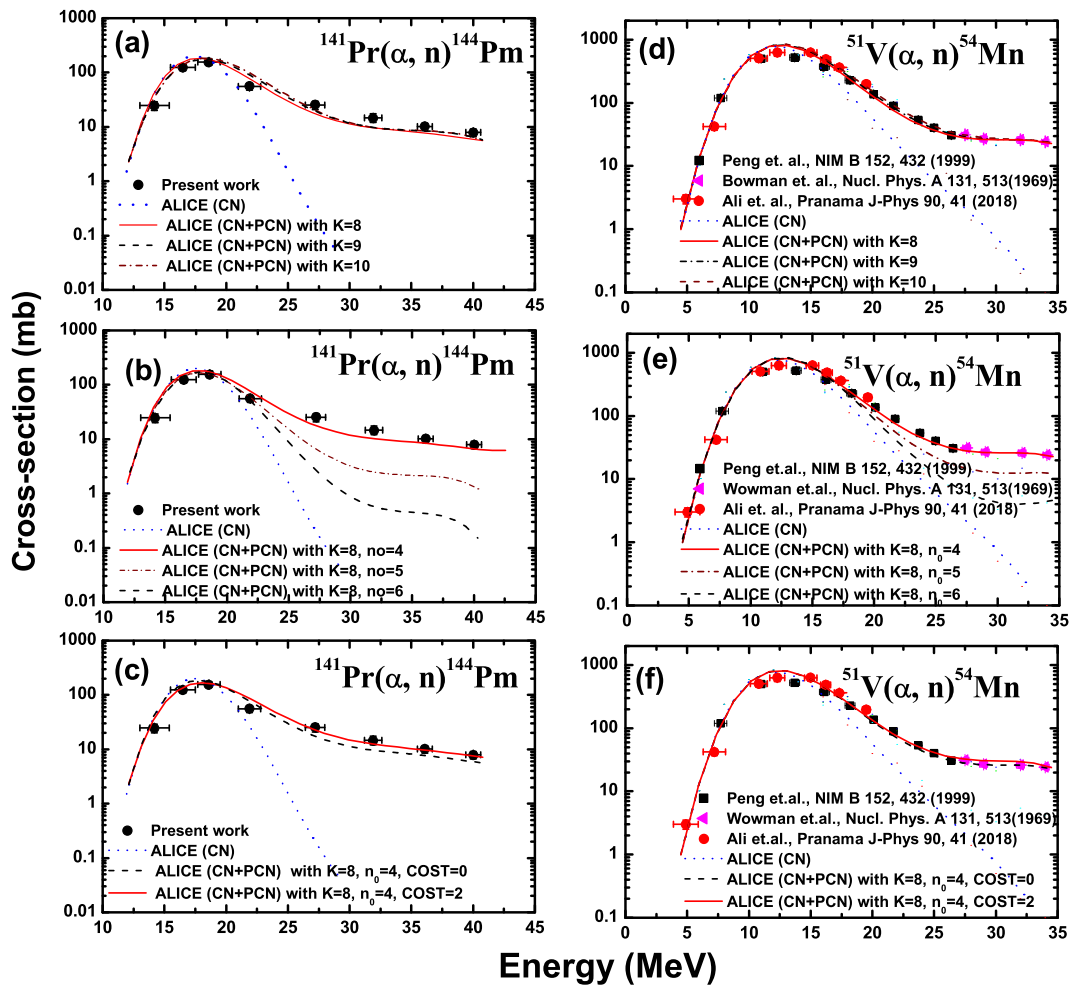


FIG. 4. (a) and (d) shows the effect of variation of parameter $K = 8, 9,$ and 10 on calculated EFs for reactions $^{141}\text{Pr}(\alpha, n)^{144}\text{Pm}$ and $^{51}\text{V}(\alpha, n)^{54}\text{Mn}$ by using code ALICE. The experimentally measured EFs are also shown in this figure. (b) and (e) shows the effect of variation of parameter $n_0 = 4, 5,$ and 6 of the code ALICE on the calculated EFs for these reactions. (c) and (f) shows the effect of variation of parameter $\text{COST} = 0$ and $\text{COST} = 2$ on calculated EFs for these reactions. These parameters used in ALICE calculations are also discussed in the text.

these figures, a value of $\text{COST} = 2$ along with $K = 8$ and $n_0 = 4$ gives best fit to the experimental data over the entire range of projectile energies.

IV. PREVIOUS EXPERIMENTAL DATA

Evidence from previous experimental work, however, suggests that the PCN process competes with CN process at a critical value of excitation energy depending on mass of target nuclei. To get systematics in α -induced reactions on various targets of odd Z and odd A , the experimental data of one neutron channel in $\alpha + ^{51}\text{V}$, $\alpha + ^{55}\text{Mn}$, $\alpha + ^{93}\text{Nb}$, $\alpha + ^{121}\text{Sb}$, and $\alpha + ^{123}\text{Sb}$ systems [1, 12, 34, 40] have also been obtained from the literature, covering mass number $A = 51$ to $A = 141$. An attempt has been made to see the effect of variation of PCN parameters on the measured EFs. The effect of variation of parameter K (8–10), initial exciton number n_0 (4–6) and mean-free path multiplier COST on the EFs for reaction $^{51}\text{V}(\alpha, n)^{54}\text{Mn}$ is shown in Figs. 4(d)–4(f), respectively. As can be seen from Figs. 4(d)–4(f) that the same set of parameters as used for reaction $^{141}\text{Pr}(\alpha, n)^{144}\text{Pm}$

is able to reproduce the measured excitation functions for reaction $^{51}\text{V}(\alpha, n)^{54}\text{Mn}$. The detailed discussion on the parameters used in the code ALICE calculations have already been presented in the previous Sec. IV of paper. Thus, these values of input parameters of the code ALICE may be considered, in general, to reproduce the experimental PCN data for target nuclei between mass number $A = 51$ to $A = 141$ for α -induced reactions on other target nuclei. The theoretical calculations performed with the same set of parameters for reactions $^{93}\text{Nb}(\alpha, n)^{96}\text{Tc}$, $^{121}\text{Sb}(\alpha, n)^{124}\text{I}$, and $^{123}\text{Sb}(\alpha, n)^{126}\text{I}$ are shown in Figs. 5(a)–5(d), respectively, along with their experimental values. It may be observed that ALICE calculations with this set of parameters ($K = 8$, $n_0 = 4$, and $\text{COST} = 2$) satisfactorily reproduce the experimental EFs for all the presently studied systems.

V. SYSTEMATICS OF THE PRECOMPOUND PROCESS

In order to obtain the systematics of precompound process, the contribution of PCN in each reaction has been deduced in the form of precompound fraction (F_{PCN})

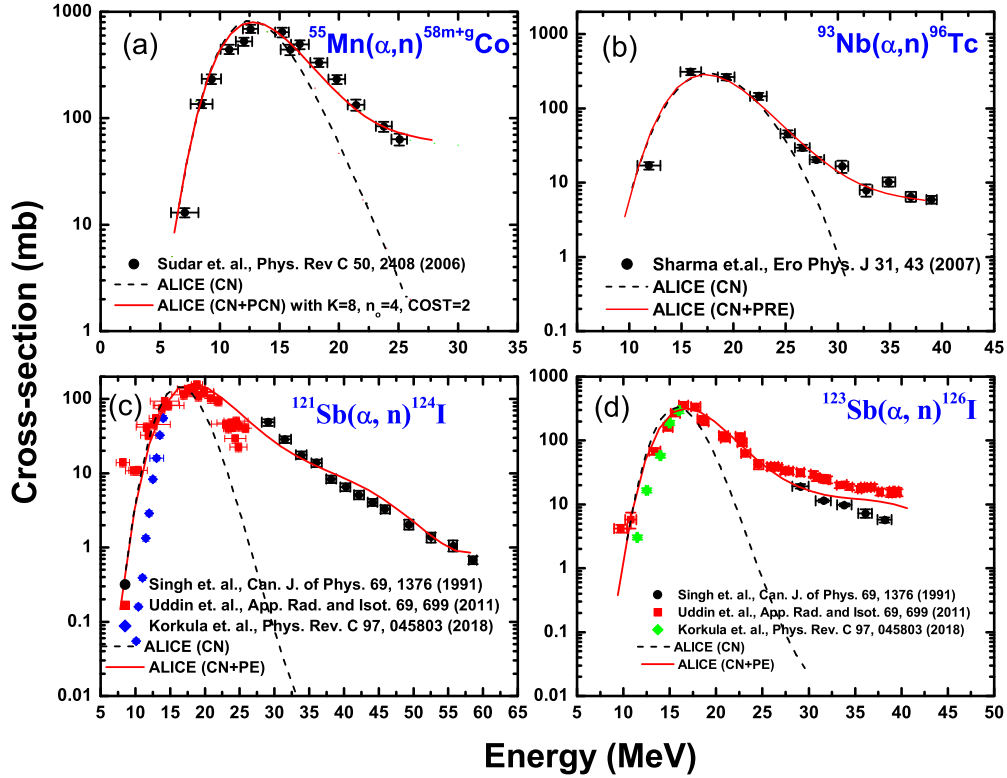


FIG. 5. The experimental and calculated EFs for reactions $^{55}\text{Mn}(\alpha, n)^{58m+g}\text{Co}$, $^{93}\text{Nb}(\alpha, n)^{96}\text{Tc}$, $^{121}\text{Sb}(\alpha, n)^{124}\text{I}$, and $^{123}\text{Sb}(\alpha, n)^{126}\text{I}$. The parameters used in ALICE calculations for these reactions are same as in Fig. 1, and are discussed in the text.

that reflects the relative importance of the PCN process over CN process. The F_{PCN} is taken as the ratio of the difference of the cross sections for (PCN+CN) emission and the CN cross sections to the cross-section values of (PCN+CN). The deduced F_{PCN} values are plotted as a function of the center-of-mass energy E_{CM} for the reactions $^{51}\text{V}(\alpha, n)^{54}\text{Mn}$, $^{55}\text{Mn}(\alpha, n)^{58m+g}\text{Co}$, $^{93}\text{Nb}(\alpha, n)^{96}\text{Tc}$, $^{121}\text{Sb}(\alpha, n)^{124}\text{I}$, $^{123}\text{Sb}(\alpha, n)^{126}\text{I}$, and $^{141}\text{Pr}(\alpha, n)^{144}\text{Pm}$, respectively, and are shown in Fig. 6. As can be seen from this figure that F_{PCN} for these reactions increases with the center of mass energy E_{CM} for each target. The small variation in E_{CM} produces a large change in F_{PCN} . The values of E_{CM} at which F_{PCN} starts and attain maximum are different for different targets. As the onset value of F_{PCN} for ^{123}Sb , ^{55}Mn , ^{121}Sb , and ^{141}Pr , lie between ^{51}V and ^{93}Nb , hence, there is no clear mass number systematics with the E_{CM} on these targets. As such E_{CM} may not be a good parameter to characterize precompound process.

Further, to see the effect of excitation energy in precompound process and to get a systematics with mass number, the values of deduced F_{PCN} are plotted as a function of the excitation energy for the reactions $^{51}\text{V}(\alpha, n)^{54}\text{Mn}$, $^{55}\text{Mn}(\alpha, n)^{58m+g}\text{Co}$, $^{93}\text{Nb}(\alpha, n)^{96}\text{Tc}$, $^{121}\text{Sb}(\alpha, n)^{124}\text{I}$, $^{123}\text{Sb}(\alpha, n)^{126}\text{I}$, and $^{141}\text{Pr}(\alpha, n)^{144}\text{Pm}$ and are shown in Fig. 7. As can be seen from this figure, the threshold value of the excitation energy at which F_{PCN} begins is lower for the heavier target ^{141}Pr and larger for light mass target ^{51}V , except for the target ^{93}Nb . The F_{PCN} for presently studied reactions attains a maximum value, that particularly depends on the mass number of the target nucleus. The higher the mass

of the target nuclei, the lower the values of the excitation energies at which maxima occurs. It means that the higher number of nucleons in the target, the lesser is the excitation energy required to attain maximum value of F_{PCN} . The lower value of the excitation energies for heavier target at which maxima in F_{PCN} is attained favors the emission of more pre-

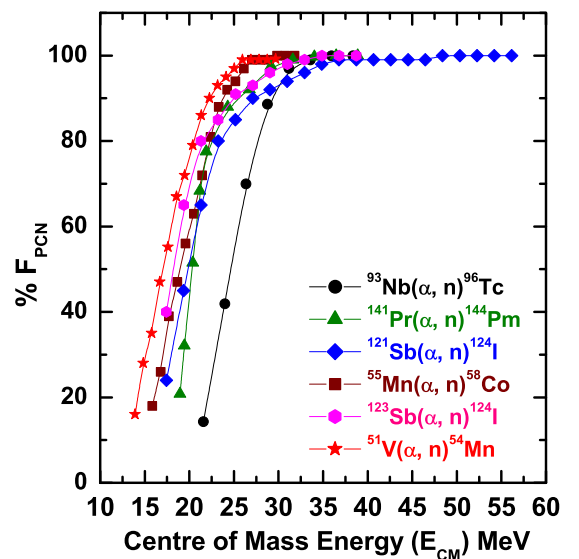


FIG. 6. The variation PCN fraction F_{PCN} as a function of center of mass energy E_{CM} for $\alpha + ^{51}\text{V}$, $\alpha + ^{55}\text{Mn}$, $\alpha + ^{93}\text{Nb}$, $\alpha + ^{121}\text{Sb}$, $\alpha + ^{123}\text{Sb}$, and $\alpha + ^{141}\text{Pr}$ systems, respectively.

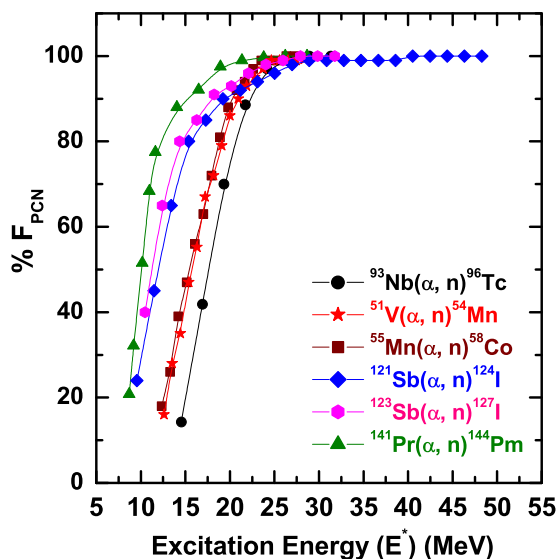


FIG. 7. The variation PCN fraction F_{PCN} as a function of excitation energy, E^* for $\alpha + {}^{51}\text{V}$, $\alpha + {}^{55}\text{Mn}$, $\alpha + {}^{93}\text{Nb}$, $\alpha + {}^{121}\text{Sb}$, $\alpha + {}^{123}\text{Sb}$, and $\alpha + {}^{141}\text{Pr}$ systems, respectively.

compound particles than that of single precompound particle. The observed inconsistency in F_{PCN} for target ${}^{93}\text{Nb}$ is rectified as discussed below.

As discussed, the deduced F_{PCN} for target ${}^{93}\text{Nb}$ does not follow the trend, therefore, no clear systematic dependence on target mass with respect to excitation energy is obtained. In order to get the systematic dependence of F_{PCN} on target mass, a more appropriate parameter, i.e., the excitation energy per surface nucleon is chosen. This is expected in the precompound emission the participation of nucleons on the surface of the composite system is more probable as compared

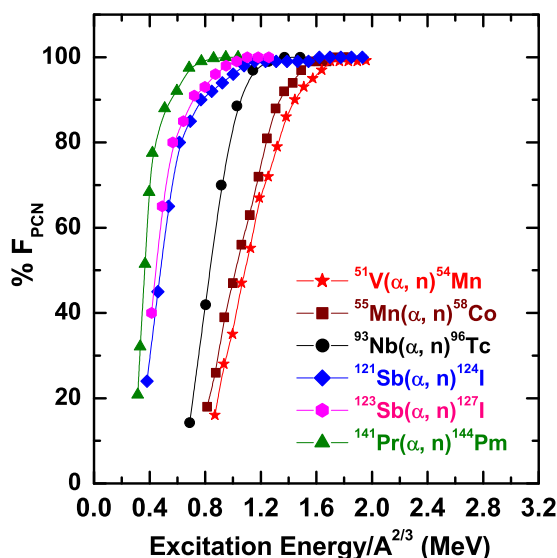


FIG. 8. The variation PCN fraction of F_{PCN} as a function of excitation energy per nucleon at the surface of the composite system, i.e., $E^*/A^{2/3}$, for $\alpha + {}^{51}\text{V}$, $\alpha + {}^{55}\text{Mn}$, $\alpha + {}^{93}\text{Nb}$, $\alpha + {}^{121}\text{Sb}$, $\alpha + {}^{123}\text{Sb}$, and $\alpha + {}^{141}\text{Pr}$ systems, respectively.

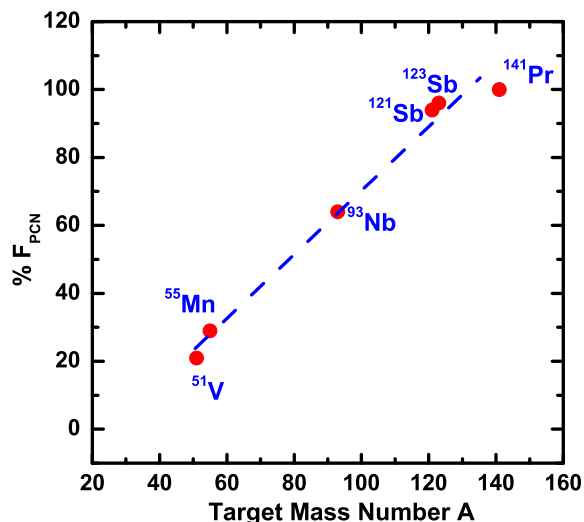


FIG. 9. A systematics developed by plotting PCN fraction F_{PCN} as a function for target mass number (A) at a fixed value of $E^*/A^{2/3}$ for $\alpha + {}^{51}\text{V}$, $\alpha + {}^{55}\text{Mn}$, $\alpha + {}^{93}\text{Nb}$, $\alpha + {}^{121}\text{Sb}$, $\alpha + {}^{123}\text{Sb}$, and $\alpha + {}^{141}\text{Pr}$ systems, respectively, (see text for details).

to the nucleons well inside, as such, the excitation energy per nucleon available at the surface of composite system ($E^*/A^{2/3}$) may be used as another important parameter to influence the PCN process. To get a systematic trend, the F_{PCN} for the above systems are plotted as a function of the $E^*/A^{2/3}$ and are shown in Fig. 8. As can be seen from this figure that a systematic trend of the F_{PCN} in terms of mass of the target nuclei and the excitation energy per nucleon at the surface of composite system is observed for all the targets studied in the present work. This may lead to an additional justification that in the precompound emission all the nucleons of the composite system are not involved in the reaction mechanism. As such, the precompound emission may have significant effect from the surface interactions. It is better to assume with the physics point of view that the particles interacting through the nuclear periphery may have a better chance to be emitted as PCN particles as compared to the particles passing through the entire diameter of the target. The conclusions drawn from above study provide a new systematics for precompound process in α -induced reactions.

The Fig. 9 depicts a linear relation between F_{PCN} and mass number A of the target nucleus at a particular value of $E^*/A^{2/3} = 0.85$ MeV, for presently studied targets. As can be seen from this figure, the F_{PCN} for the presently studied systems linearly increases with mass of the targets. It may also be concluded from this figure that as mass number approaches towards $A = 141$, the one-neutron emission probability is entirely through precompound emission. As such, the systematics obtained from the present analysis is interesting and throw an additional insight on our existing understanding to the precompound emission process.

VI. CONCLUSIONS

A detailed analysis of excitation functions has been performed to investigate the systematics of precompound process

with mass number of target nuclei. The analysis of excitation function data for $\alpha + {}^{51}\text{V}$, $\alpha + {}^{55}\text{Mn}$, $\alpha + {}^{93}\text{Nb}$, $\alpha + {}^{121}\text{Sb}$, $\alpha + {}^{123}\text{Sb}$, and $\alpha + {}^{141}\text{Pr}$ systems indicates that experimental excitation functions could be reproduced only when the precompound emission, is taken into account in theoretical calculations. It has been observed that the same set of precompound parameters of the code ALICE satisfactorily reproduces the experimental existing EFs data for all the presently studied systems that may further be used to develop a systematics in α -induced reactions. The systematics deduced for PCN process from the measurements and analysis of EFs data indicates that precompound fraction sensitively depends on

the excitation energy per surface nucleon ($E^*/A^{2/3}$) of the composite systems and mass number of the target nuclei. As such, it may be concluded that surface nucleons play a significant role in precompound emission.

ACKNOWLEDGMENTS

The authors are thankful to the Director, VECC, Kolkata, India for extending all the facilities for carrying out the experiments. One of the authors M.K.S. thanks the Council of Scientific and Industrial Research (CSIR), New Delhi (Project No. 03(361)16/EMR-11 for financial support.

-
- [1] B. P. Singh, H. D. Bhardwaj, and R. Prasad, *Can. J. Phys.* **69**, 1376 (1991).
- [2] E. Holub, D. Pocanic, R. Caplar, and N. Cindro, *Z. Physik A - Atoms and Nuclei* **296**, 341 (1980).
- [3] M. Herman, A. Marcinkowski, and K. Stankiewicz, *Nucl. Phys. A* **430**, 69 (1984).
- [4] M. Herman, G. Reffo, and C. Costa, *Phys. Rev. C* **39**, 1269 (1989).
- [5] H. Feshbach, *Rev. Mod. Phys.* **46**, 1 (1974).
- [6] H. Feshbach, A. Kerman, and S. Koonin, *Ann. Phys. (NY)* **125**, 429 (1980).
- [7] B. P. Singh, M. G. V. Sankaracharyulu, M. A. Ansari, H. D. Bhardwaj, and R. Prasad, *Phys. Rev. C* **47**, 2055 (1993).
- [8] B. P. Singh, M. G. V. Sankaracharyulu, M. A. Ansari, H. D. Bhardwaj, and R. Prasad, *Int. J. Mod. Phys. E* **1**, 823 (1991).
- [9] A. Agarwal, M. K. Bhardwaj, I. A. Rizvi, and A. K. Chaubey, *J. Phys. Soc. Jpn.* **70**, 2903 (2001).
- [10] M. Avrigeanu, V. Avrigeanu, P. Bém, U. Fischer, M. Honusek, K. Katovsky, C. Mănăilescu, J. Mrázek, E. Šimečková, and L. Závorka, *Phys. Rev. C* **89**, 044613 (2014).
- [11] K. Kim, G. N. Kim, H. Naik, M. Zaman, S.-C. Yang, T.-Y. Song, R. Guin, and S. K. Das, *Nucl. Phys. A* **935**, 65 (2015).
- [12] M. K. Sharma, H. D. Bhardwaj, Unnati, P. P. Singh, B. P. Singh, and R. Prasad, *Eur. Phys. J.* **31**, 43 (2007).
- [13] B. P. Singh, Manoj K. Sharma, M. M. Muthafa, H. D. Bhardwaj, and R. Prasad, *Nucl. Instrum. Meth. Phys. Res. A* **562**, 717 (2006).
- [14] J. Pal, S. Saha, C. C. Dey, P. Banerjee, S. Bose, B. K. Sinha, M. B. Chatterjee, and S. K. Basu, *Phys. Rev. C* **71**, 034605 (2005).
- [15] S. Mukherjee, N. L. Singh, G. K. Kumar, and L. Chaturvedi, *Phys. Rev. C* **72**, 014609 (2005).
- [16] K. F. Hassan, S. M. Qaim, Z. A. Saleh, and H. H. Coenen, *Appl. Rad. Isotopes* **64**, 101 (2006).
- [17] B. P. Singh, H. D. Bhardwaj, and R. Prasad, *Il Nuovo Cimento* **104A**, 45 (1991).
- [18] A. J. Koning and J. M. Akkermans, *Phys. Rev. C* **47**, 724 (1993).
- [19] S. S. Dimitrova, A. A. Cowley, E. V. Zemlyanaya, and K. V. Lukyanov, *Phys. Rev. C* **90**, 054604 (2014).
- [20] J. R. Wu, C. C. Chang, and H. D. Holmgren, *Phys. Rev. C* **19**, 698 (1979).
- [21] T. C. Awes, G. Poggi, C. K. Gelbke, B. B. Back, B. G. Glagola, H. Breuer, and V. E. Viola, *Phys. Rev. C* **24**, 89 (1981).
- [22] J. Luo, L. Jiang, and S. Li, *Phys. Rev. C* **96**, 044617 (2017).
- [23] M. K. Sharma, P. P. Singh, D. P. Singh, A. Yadav, V. R. Sharma, I. Bala, R. Kumar, A. Yadav, B. P. Singh, and R. Prasad, *Phys. Rev. C* **91**, 014603 (2015).
- [24] K. Maeda, H. Ejiri, T. Shibata, K. Okada, T. Motobayashi, M. Sasao, T. Kishimoto, H. Suzuki, H. Sakai, and A. Shimizu, *Nucl. Phys. A* **379**, 160 (1982).
- [25] T. Kishimoto, M. Sasao, H. Suzuki, H. Sakai, and H. Ejiri, *Nucl. Phys. A* **337**, 493 (1980).
- [26] H. Sakai, A. Shimizu, H. Ejiri, T. Shibata, K. Okada, T. Kishimoto, and K. Maeda, *Phys. Rev. C* **22**, 1002 (1980).
- [27] L. Westerberg, D. G. Sarantites, D. C. Hensley, R. A. Dayras, M. L. Halbert, and J. H. Barker, *Phys. Rev. C* **18**, 796 (1978).
- [28] D. G. Sarantites, L. Westerberg, M. L. Halbert, R. A. Dayras, D. C. Hensley, and J. H. Barker, *Phys. Rev. C* **18**, 774 (1978).
- [29] D. G. Sarantites, L. Westerberg, R. A. Dayras, M. L. Halbert, D. C. Hensley, and J. H. Barker, *Phys. Rev. C* **17**, 601 (1978).
- [30] E. Gadioli, E. Gadioli-Ebra, J. J. Hogan, and B. V. Jacab, *Phys. Rev. C* **29**, 76 (1984).
- [31] J. Ernst, W. Friedland, and H. Stockhorst, *Z. Phys. A - Atomic Nuclei* **328**, 333 (1987).
- [32] J. Ernst, W. Friedland, and H. Stockhorst, *Z. Phys. A - Atomic Nuclei* **308**, 301 (1982).
- [33] S. Sudar and S. M. Qaim, *Phys. Rev. C* **73**, 034613 (2006).
- [34] X. Peng, F. He, and X. Long, *Nucl. Instrum. Meth. Phys. Res. B* **152**, 432 (1999).
- [35] C. Rubbia, J. A. Rubbio, S. Buono *et al.*, Conceptual Design of a Fast Neutron Operated High Power Energy Amplifier, Report CERN/AT/95-94 (ET), 1995.
- [36] R. da Silveira and C. Leclercq-Willain, *Phys. Rev. C* **70**, 044604 (2004).
- [37] P. P. Singh *et al.*, *Phys. Rev. C* **80**, 064603 (2009); **78**, 017602 (2008).
- [38] D. P. Singh, Unnati, P. P. Singh, A. Yadav, M. K. Sharma, B. P. Singh, K. S. Golda, R. Kumar, A. K. Sinha, and R. Prasad, *Phys. Rev. C* **81**, 054607 (2010).
- [39] Mohd. Shuaib *et al.*, *Phys. Rev. C* **94**, 014613 (2016); *J. Phys. G: Nucl. Part. Phys.* **44**, 105108 (2017); *Phys. Rev. C* **98**, 014605 (2018).
- [40] W. W. Bowman and M. Blann, *Nucl. Phys. A* **131**, 513 (1969).
- [41] B. M. Ali *et al.*, *Pramana J. Phys.* **90**, 41 (2018).
- [42] S. Sudar and S. M. Qaim, *Phys. Rev. C* **50**, 2408 (1994).
- [43] M. S. Uddin, A. Hermanne, S. Sudar, M. N. Aslam, B. Scholten, H. H. Coenen, and S. M. Qaim, *Appl. Rad. Isotopes* **69**, 699 (2011).
- [44] Z. Korkulu, N. Özkan, G. G. Kiss *et al.*, *Phys. Rev. C* **97**, 045803 (2018).
- [45] M. Blann, Report PSR-146 NEA Data Bank, Gif-sur-Yvette, France, 1991.
- [46] V. F. Weisskopf and D. H. Ewing, *Phys. Rev.* **57**, 472 (1940).

- [47] M. Blann, *Phys. Rev. Lett.* **28**, 757 (1972).
- [48] The Stopping and Range of Ions in Matter (SRIM) code, <http://www.srim.org/SRIM/SRIMLEGL.htm>
- [49] E. Browne and R. B. Firestone, *Table of Radioactive Isotopes* (Wiley, New York, 1986).
- [50] R. B. Firestone and V. S. Shirley, *Table of Isotopes*, 8th ed., (Wiley, New York, 1996).
- [51] E. Storm *et al.*, Table of γ -ray absorption coefficients for elements 1 through 100, LA-2237, 65 (1958).
- [52] W. D. Myers and W. J. Swiatecki, *Ark. Phys.* **36**, 343 (1967).
- [53] F. D. Becchetti and G. W. Greenlees, *Phys. Rev.* **182**, 1190 (1969).
- [54] K. Kikuchi and M. Kawai, *Nuclear Matter and Nuclear Reactions* (North-Holland, Amsterdam, 1968).
- [55] M. Blann, *Nucl. Phys. A* **213**, 570 (1973).
- [56] M. Blann and H. K. Vonach, *Phys. Rev. C* **28**, 1475 (1983); M. Blann and J. Bisplinghoff, Lawrence Livermore National Laboratory Report No. UCID 19614, 1983 (unpublished).
- [57] W. Dilg, W. Schantl, and H. Vonach, *Nucl. Phys. A* **217**, 269 (1973).